PALEOBIOLOGY
A PUBLICATION OF THE Paleontological SOCIETY

Featured Article

Convergence and constraint in the cranial evolution of mosasaurid reptiles and early cetaceans

Rebecca F. Bennion ⬡, Jamie A. MacLaren, Ellen J. Coombs, Felix G. Marx*,
Olivier Lambert ⬡, and Valentin Fischer*

Abstract.—The repeated return of tetrapods to aquatic life provides some of the best-known examples of convergent evolution. One comparison that has received relatively little focus is that of mosasaurids (a group of Late Cretaceous squamates) and archaic cetaceans (the ancestors of modern whales and dolphins), both of which show high levels of craniodental disparity, similar initial trends in locomotory evolution, and global distributions. Here we investigate convergence in skull ecomorphology during the initial aquatic radiations of these groups. A series of functionally informative ratios were calculated from 38 species, with ordination techniques used to reconstruct patterns of functional ecomorphospace occupation. The earliest fully aquatic members of each clade occupied different regions of ecomorphospace, with basilosaurids and early russellosaurines exhibiting marked differences in cranial functional morphology. Subsequent ecomorphological trajectories notably diverge: mosasaurids radiated across ecomorphospace with no clear pattern and numerous reversals, whereas cetaceans notably evolved toward shallower, more elongated snouts, perhaps as an adaptation for capturing smaller prey. Incomplete convergence between the two groups is present among megapredatory and longirostrine forms, suggesting stronger selection on cranial function in these two ecomorphologies. Our study highlights both the similarities and divergences in craniodental evolutionary trajectories between archaic cetaceans and mosasaurids, with convergences transcending their deeply divergent phylogenetic affinities.

Rebecca F. Bennion. Evolution & Diversity Dynamics Lab, Université de Liège, Liège, Belgium; and Operational Directorate of Earth and History of Life, Institut royal des Sciences naturelles de Belgique, Brussels, Belgium. E-mail: r.bennion@uliege.be

Jamie A. MacLaren. Evolution & Diversity Dynamics Lab, Université de Liège, Liège, Belgium and Functional Morphology Lab, Department of Biology, Universiteit Antwerpen, Antwerp, Belgium. E-mail: j.maclaren@uliege.be

Ellen J. Coombs[†]. Department of Life Sciences, Natural History Museum, London, U.K.; and Genetics, Evolution, and Environment Department, University College London, London, U.K. E-mail: ellen.coombs.14@ucl.ac.uk. [†]Present address: Department of Vertebrate Zoology, National Museum of Natural History, Smithsonian Institution, Washington D.C., U.S.A.

Felix G. Marx. Museum of New Zealand Te Papa Tongarewa, Wellington, New Zealand; and Department of Geology, University of Otago, Dunedin, New Zealand. E-mail: felix.marx@tepapa.govt.nz

Olivier Lambert. Operational Directorate of Earth and History of Life, Institut royal des Sciences naturelles de Belgique, Brussels, Belgium. E-mail: olambert@naturalsciences.be

Valentin Fischer. Evolution & Diversity Dynamics Lab, Université de Liège, Liège, Belgium. E-mail: v.fischer@uliege.be

Introduction

Over their 390 Myr history, more than 60 lineages of tetrapods have independently reinvaded aquatic ecosystems (Vermeij and Motani 2018). The shared constraints they faced as part of this transition led to many textbook examples of evolutionary convergence in terms of feeding ecology, sensory biology, and locomotion, among others (Kelley and Pyenson 2015). One comparison that has received relatively little attention is that between archaic cetaceans (the Eocene and

0094-8373/23

Oligocene ancestors of modern whales, dolphins, and porpoises) and mosasaurids (a clade of Late Cretaceous marine squamates). Both groups show similar raptorial ecomorphotypes, such as putative megapredators (Gallagher 2014; Voss et al. 2019); changes in postcranial anatomy, such as loss of sacral attachment and changes in limb morphology (Uhen 2010; Lindgren et al. 2011); and a shift from axial propulsion in the form of undulation to more efficient locomotion based on caudal oscillation (Buchholtz 2001; Lindgren et al. 2010, 2011).

The earliest fully aquatic cetaceans (the basilosaurid lineage of archaeocetes) existed for more than 7 Myr before giving rise to the two neocete groups that survive to the present day: the odontocetes (toothed whales) and the mysticetes (baleen whales) (Lambert et al. 2017; Coombs et al. 2022). Mosasaurids, on the other hand, diversified into three parallel lineages early on in their evolutionary history (Russellosaurina, Mosasaurinae, and the more basal Halisaurinae), and radiated in a series of different waves until their extinction at the Cretaceous/Paleogene (K/Pg) boundary (Everhart 2005). Both mosasaurids and early cetaceans ultimately achieved near global distributions (Polcyn et al. 2014; Buono et al. 2019), high levels of taxonomic diversity (Polcyn et al. 2014; Marx and Fordyce 2015), and notable craniodental disparity (Fitzgerald 2010; Boessenecker et al. 2017b; Coombs et al. 2022; Cross et al. 2022; MacLaren et al. 2022).

Despite being frequently cited as a classic example of evolutionary convergence (Kelley and Pyenson 2015), similarities in ecomorphology between extinct marine tetrapods have only recently begun to be investigated using rigorous quantitative methods. Much of the focus of this research has been on cranial and dental morphology due to the wealth of fossilized remains and the ecological information that can be extracted (Kelley and Motani 2015; Motani et al. 2015; Stubbs and Benton 2016; Fischer et al. 2017; Reeves et al. 2021; Cross et al. 2022). In this paper, we quantitatively analyze cranial evolution in mosasaurids and early (fully aquatic) cetaceans during the first ca. 20 Myr of their evolutionary histories. We explicitly test for possible instances of ecomorphological convergence in the skulls and teeth between the groups; based on previous qualitative comparisons (Gallagher 2014; Kelley and Pyenson 2015), we predict a high level of convergence between megapredatory mosasaurids (e.g., *Mosasaurus*, *Tylosaurus*) and basilosaurid archaeocetes. In addition, we anticipate high convergence scores between putative small-prey specialists with an elongate snout. Finally, previous studies have suggested that the shift from axial-based to caudal-based locomotion resulted in increased efficiency and more effective colonization of open-ocean niches (Fish 2001; Lindgren et al. 2011), with ramifications for feeding and sensory ecology; we therefore hypothesize that skull ecomorphology will exhibit trajectory shifts with the acquisition of new locomotor techniques.

Institutional Abbreviations.—CCNHM, Mace Brown Museum College of Charleston, Charleston, South Carolina, U.S.A.; ChM, the Charleston Museum, Charleston, South Carolina, U.S.A.; FHSM, Fort Hays State University Sternberg Museum of Natural History, Hays, Kansas, U.S.A.; FMNH, Field Museum Chicago, Chicago, Illinois, U.S.A.; HUJ, Hebrew University of Jerusalem, Israel; IRSNB, Institut Royal des Sciences Naturelles de Belgique, Brussels, Belgium; KUVP, University of Kansas Natural History Museum, Lawrence, Kansas, U.S.A.; MHNM, Museum of Natural History of Marrakech at Cadi Ayyad University, Marrakech, Morocco; MNHN, Muséum National d'histoire Naturelle, Paris, France; MUSM, Museo de Historia Natural, Universidad Nacional Mayor de San Marcos, Lima, Peru; NMV, National Museums Victoria, Melbourne, Australia; OU, University of Otago, Dunedin, New Zealand; SMU, Shuler Museum of Paleontology, Southern Methodist University, Dallas, Texas, U.S.A.; TATE, Tate Geological Museum, Casper, Wyoming, U.S.A.; TMP, Royal Tyrrell Museum of Palaeontology, Drumheller, Alberta, Canada; UALVP, University of Alberta Laboratory for Vertebrate Palaeontology, Edmonton, Canada; UCMP, Museum of Paleontology, University of California, Berkeley, California, U.S.A.; UMMP, University of Michigan Museum of Palaeontology, Ann Arbor, Michigan, U.S.A.; UMORF, the University of Michigan Online Repository of

Fossils; USNM, U.S. National Museum of Natural History, Smithsonian Institution, Washington, D.C., U.S.A.

Methods

Data Sampling.—Our analyses focus on the skulls of 21 mosasaurid species (1 halisaurine, 11 russellosaurines, and 9 mosasaurines) and 17 cetacean species (4 archaeocetes, 5 toothed mysticetes, and 8 odontocetes) (Table 1). The Oligocene cetacean *Kekenodon* has uncertain phylogenetic affinities; we follow previous work in placing the taxon as sister to the Neocete node (Clementz et al. 2014) and group it in our analyses with the other archaeocetes belonging to the family Basilosauridae. We took 12 linear measurements of each skull and jaw, either directly on the specimen or from high-precision 3D models (Fig. 1). Where neither option was available, measurements were taken from figured specimens using ImageJ (v. 1.53), and these data were cross-checked using other photographs and information from associated papers. We used our measurements to calculate 10 morphofunctional ratios with well-established functional and biomechanical outcomes, for example, mechanical advantage for jaw adduction calculated from mandibular lever arms (Anderson et al. 2011; Table 2). Functional ratios were adapted from previous studies (Anderson et al. 2011; Stubbs and Benton 2016; MacLaren et al. 2017; Fischer et al. 2020) and selected specifically to enable viable comparisons between mosasaurids and cetaceans (Supplementary Material).

To place our results into ecological context, we searched the literature for observations and evidence regarding the feeding and locomotor ecology of our study species (Supplementary Tables 1, 2). Given the breadth of taxa in this dataset, as well as inevitable uncertainties on paleoecology and life history for fossil species, we used relatively broad categories of diet (apex, fish/squid, benthic) and locomotion (anguilliform, sub-carangiform, and carangiform) following published studies (Pauly et al. 1998; Kelley and Motani 2015; Gutarra and Rahman 2022). Inferences about feeding ecology were not based on morphological information considered in our dataset so as to avoid circular reasoning; rather, we considered preserved stomach contents and craniodental features such as tooth wear, which fell outside the scope of our measurements.

Ecomorphospace Occupation, Phylogeny, and Disparity.—All analyses were carried out in the statistical software R v. 4.1.0 (R Core Team 2021). The ecomorphological dataset was passed through a completeness threshold of 45% per taxon, then z-transformed and converted to a Euclidian distance matrix. Pairwise biplots and correlations between all traits were computed using the psych v. 2.1.3 package. We employed two different types of ordination: (1) principal coordinates analysis (PCoA) using the ape v. 5.5 package, applying the Caillez correction for negative eigenvalues (Paradis et al. 2004); and (2) nonmetric multidimensional scaling (NMDS), using the vegan v. 2.5-7 package (Oksanen et al. 2007), with two dimensions predefined. NMDS is better for visualizing morphospace (as it can account for all variation in two axes); however, as it is nonmetric and cannot be used for statistical analyses, PCoA was also computed for quantitative use.

Skull size is an important factor in marine vertebrate ecology (McCurry et al. 2017b), and here we visualize it via two proxy measurements: skull length (commonly used for marine reptiles) and bizygomatic width, here defined as the maximum distance between the outer edges of the squamosals (commonly used in cetaceans) (Pyenson and Sponberg 2011). In an attempt to assimilate marine reptile and cetacean datasets, we chose to employ both measurements. Size was used here for scaling data points in ordination analyses; it was not used as an independent ecomorphological trait in itself. The natural logarithm of size metrics was used to explore frequency of different-sized taxa within and between the two groups.

We created a phylomorphospace to visualize ecomorphological trends across the evolution of both groups and test for convergence. Our composite tree combines recently published topologies for cetaceans and mosasaurids (Martínez-Cáceres et al. 2017; Strong et al. 2020). Taxa not included in these studies were grafted on the phylogeny using the phytools v. 0.7-80 and paleotree v. 3.3.25 packages (Bapst 2012; Revell 2012), based on their

TABLE 1.   List of specimens used and data sources. Institutional abbreviations are provided in the main text.

Taxon	Specimen	Clade	Age range (Ma)	Source of measurements	3D model location (if applicable)
Cynthiacetus peruvianus	MNHN F PRU10 (cast at IRSNB)	Basilosaurid archaeocete	41.3–33.9	3D model	Morphosource Project 000391764
Dorudon atrox	UMMP VP 118183	Basilosaurid archaeocete	41.3–33.9	3D model, measured online	UMORF
Basilosaurus isis	UMMP VP 118204	Basilosaurid archaeocete	41.3–33.9	3D model, measured online	UMORF
Kekenodon sp.	OU 22294	Archaeocete	27.3–25.2	3D model	Specimen currently being described—contact curators.
Mystacodon selenensis	MUSM 1917	Mysticete	38–33.9	3D model	Morphosource Project 000391764
Coronodon havensteini	CCNHM 108	Mysticete	33.9–28.1	3D model	Skull—CCNHM Sketchfab Mandible—Morphosource Project 000391764
Janjucetus hunderi	NMV P216929 (cast at MNHN)	Mysticete	28.1–23.03	3D model	Morphosource Project 000391764
Aetiocetus weltoni	UCMP 122900	Mysticete	28.1–23.03	3D model	Morphosource Project 000391764
Aetiocetus cotylalveus	USNM 25210	Mysticete	33.9–23.03	3D model	Morphosource Project 000391764
Simocetus rayi	USNM 256517	Odontocete	33.9–23.03	3D model	Morphosource Project 000391764
Agorophius sp.	CCNHM 204	Odontocete	33.9–23.03	3D model	Specimen currently being described—contact curators.
Cotylocara macei	CCNHM 101	Odontocete	28.1–23.03	3D model	CCNHM Sketchfab
Waipatia maerewhenua	OU 22095 (cast at IRSNB)	Odontocete	27.3–25.2	3D model	Morphosource Project 000391764
Ankylorhiza tiedemani	CCNHM 103	Odontocete	33.9–13.82	3D model	Morphosource Project 000391764
Xenorophus sp.	CCNHM 168	Odontocete	28.1–20.44	3D model	Specimen currently being described—contact curators.
Eosqualodon sp.	CCNHM 170	Odontocete	28.1–20.44	3D model	Specimen currently being described—contact curators.
OU 22397	OU 22397	Odontocete	28.4–23.03	3D model	Specimen currently being described—contact curators.

| *Halisaurus arambourgi* | UALVP 56123 | Halisaurine | 70.6–66 | Photographs (Jiménez-Huidobro et al. 2017) | |
Russellosaurus coheni	SMU 73056	Russellosaurine	93.5–89.3	3D model; CT scan data provided by Mike Polcyn (Polcyn and Bell 2005), model reconstructed by authors.	Morphosource Project 000391764
Tethysaurus nopcsai	MNHN 1999 9 GOU1	Russellosaurine	93.5–89.3	3D model	Morphosource Project 000391764
Ectenosaurus clidastoides	FHSM VP401	Russellosaurine	86.3–72.1	3D model	Morphosource Project 000391764
Selmasaurus johnsoni	FHSM VP13910	Russellosaurine	85.8–70.6	3D model; specimen reconstructed by authors	Morphosource Project 000391764
Platecarpus tympaniticus	KUVP 1007	Russellosaurine	89.3–70.6	3D model	Morphosource Project 000391764
Plesioplatecarpus planifrons	FHSM VP2181	Russellosaurine	86.3–85.8	3D model	Morphosource Project 000391764
Plioplatecarpus sp.	TATE VOO87	Russellosaurine	83.6–66	3D model	Morphosource Project 000391764
Tylosaurus proriger	FHSM VP3	Russellosaurine	85.8–72.1	3D model	Morphosource Project 000391764
Tylosaurus bernardi	IRSNB R23A	Russellosaurine	83.5–66	3D model	Morphosource Project 000391764
Tylosaurus nepaeolicus	FHSM VP2295	Russellosaurine	89.3–85.8	3D model	Morphosource Specimen 000S26455
Gavialimimus almaghribensis	MHNM KHG 1231	Russellosaurine	70.6–66	Photographs (Strong et al. 2020)	
Clidastes sp.	USNM 11719	Mosasaurine	86.3–72.1	3D model	Morphosource Project 000391764
Mosasaurus sp. (aff. *hoffmanni*; Lingham-Soliar 1995; Street 2016)	IRSNB R303 (formerly IRSNB R12)	Mosasaurine	72.1–66	3D model	Morphosource Project 000391764
Mosasaurus missouriensis	KUVP 1034	Mosasaurine	83.5–72.1	3D model	Morphosource Project 000391764
Mosasaurus lemonnieri	IRSNB R376	Mosasaurine	83.5–66	3D model	Morphosource Project 000391764
Globidens dakotensis	FMNH PR846	Mosasaurine	83.5–70.6	3D model	Morphosource Project 000391764
Prognathodon solvayi	IRSNB R33b	Mosasaurine	72.1–66	3D model; specimen reconstructed by authors	Morphosource Project 000391764
Prognathodon overtoni	TMP 2002.400.0001	Mosasaurine	83.5–72.1	Photographs (Konishi et al. 2011)	
Prognathodon currii	HUJ OR 100	Mosasaurine	83.5–66	Photographs (Christiansen and Bonde 2002)	
Plotosaurus bennisoni	UCMP 32778	Mosasaurine	72.1–66	3D model	Phenome10k
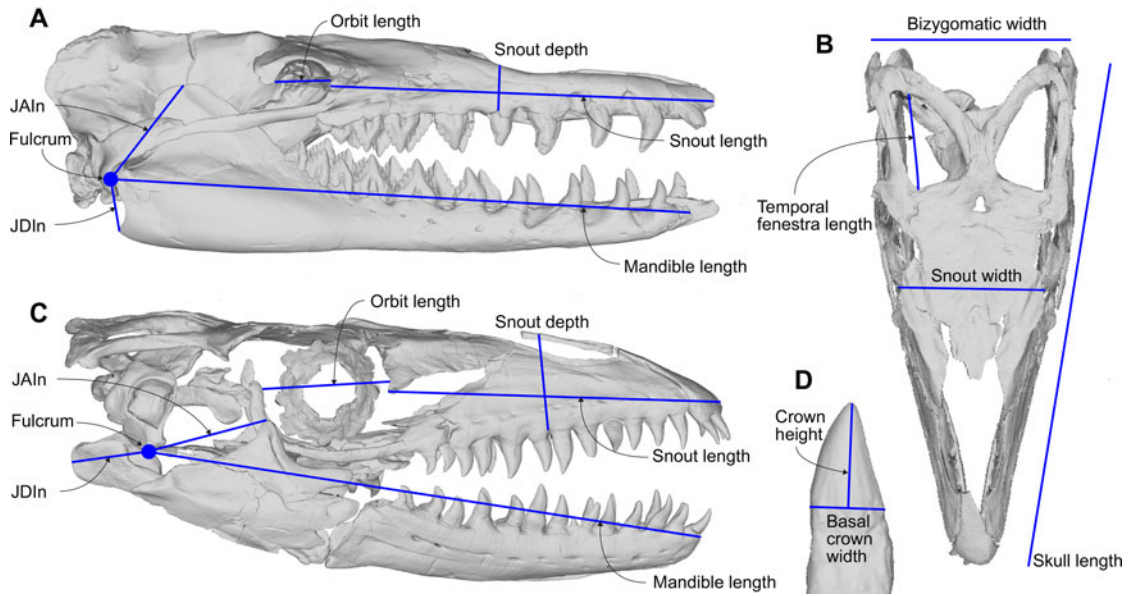
FIGURE 1.   Measurements used to calculate ecomorphological ratios, shown on the 3D models of the cetacean *Cynthiacetus peruvianus* in lateral view (A) and the skull of the mosasaurid *Prognathodon solvayi* in (B) dorsal view, (C) lateral view, and (D) labial view of a tooth from the left dentary. JAIn, jaw adductor inlever; JDIn, jaw depressor inlever.

placements in the following studies: *Mosasaurus* sp. (IRSNB R303) and *Mosasaurus lemonnieri* as sister lineages to *Mosasaurus hoffmanni* (Street 2016), *Halisaurus arambourgi* as grouped with other species of *Halisaurus* (Polcyn et al. 2012), *Coronodon havensteini* as sister lineage to *Mammalodon* (Geisler et al. 2017), *Ankylorhiza tiedemani* as sister lineage to *Agorophius* (Boessenecker et al. 2020), *Eosqualodon* sp. as sister lineage to *Squalodon* (Muizon 1991), undescribed Oligocene odontocete OU 22397 as sister lineage to *Waipatia* (Coste et al. 2018), an undescribed species of *Xenorophus* (called *Xenorophus* sp.), as sister lineage to *Xenorophus sloani* (Boessenecker et al. 2017a), *Cotylocara macei* as sister lineage to *Echovenator* (Geisler et al. 2014), and *Kekenodon* sp. as sister lineage to Mysticeti + Odontoceti (Clementz et al. 2014; Fig. 2A). We then dropped all tips for which we have insufficient (i.e., not passing the completeness threshold) or no data, using the ape v. 5.6-2 package (Paradis et al. 2004). The resulting tree was time-scaled using the minimum branch length algorithm (minimum = 3 Myr), using the paleotree v. 3.3.25 package (Bapst 2012). The temporal data were obtained from the Paleobiology Database. For the

undescribed OU 22397 (Coste et al. 2018), we used the dates of the Chattian stage of the Oligocene. The Paleobiology Database entries for two mosasaurs (*Platecarpus tympaniticus* and *Plioplatecarpus*) had outlying data points based on isolated teeth, which we chose to remove, as they extended their respective temporal ranges by more than 10 Myr. The oldest age of the range was used to calibrate the tree (dateTreatment="firstLast" argument in the timePaleoPhy function). The root was then manually increased to ensure a mid-Carboniferous (318 Ma) split between Reptilia and Synapsida (Brocklehurst et al. 2022).

Disparity (both sum of ranges and sum of variances) was calculated via the dispRity v. 1.6.1 package (Guillerme 2018) for both cetaceans and mosasaurids, as well as for major subclades (Russellosaurina, Mosasaurinae, Halisaurinae, Basilosauridae, Odontoceti, and Mysticeti), without rarefaction. All PCoA axes were used to calculate disparity, as the loadings on each axis are low.

Convergence Analyses.—Upon reviewing the results of ordination analyses, we chose a number of taxon pairs to be tested for inter- and intraclade ecomorphological convergence

TABLE 2. Measurements and ratios used in analyses.

Ratio	Calculation
Tooth shape	Tooth crown height:crown base width
Absolute tooth crown size	Tooth crown height raw measurement
Relative orbit diameter	Orbit diameter:skull length
Relative snout length	Snout length:skull length
Relative snout depth	Snout depth at the midpoint:snout length
Relative snout width	Snout width just before orbit:snout length
Anterior mechanical advantage	Distance between fulcrum and coronoid process:distance between fulcrum and anterior tip of dentary tooth row (mandible length)
Opening mechanical advantage	Distance between fulcrum and retroarticular process (mosasaurs)/ angular process (cetaceans):distance between fulcrum and anterior tip of dentary tooth row (mandible length)
Relative temporal musculature	Temporal fenestra length:skull length

(Table 3). We applied the C1 metric of Stayton (2015), which compares the morphological distance of two taxa with the morphological distance between their respective ancestral nodes, and thus quantifies how much of this difference has been lost through putative evolutionary convergence. A C1 value closer to 1 indicates greater convergence (Grossnickle et al. 2020). We used the first two PCoA axes (17.9% of variation) and all axes (100% of variation), with significance tested using the convevol v. 1.3 package (Stayton 2014) using 1000 Brownian simulations of character evolution for each pair. To test for the influence of long branches, we also ran these tests with the node determined by the minimum branch length (i.e., divergence in the Aptian).

Results

Morphological Evolution.—The earliest mosasaurids in our sample, the Turonian russellosaurines *Russellosaurus* and *Tethysaurus*, had small, relatively gracile skulls (Fig. 2B), likely limiting their diet to small prey items. Later russellosaurines and all mosasaurines radiate throughout the ecomorphospace, with no clear trajectory (Fig. 2B). Several back-and-forth occupations of novel and more ancestral phenotypes are observed; for example, the early mosasaurine *Clidastes* and the later (and larger) mosasaurine *Plotosaurus* both exhibit more longirostrine skulls with elongate teeth and a relatively small area of temporal musculature (Fig. 2B). Ecomorphological variation is present within genera with multiple species, such as *Mosasaurus* and *Prognathodon* (Fig. 2B).

Mosasaurid apex predators like *Prognathodon*, *Mosasaurus*, and *Tylosaurus* are split into two distinct regions of ecomorphospace, with *Prognathodon* exhibiting more robust snout and mandibles, indicating higher stress-resistance during biting in this genus (Fig. 2B). The durophagous mosasaurid *Globidens dakotensis* is not separate from other mosasaurids, rather plotting among the large apex predators (Fig. 2B). In both the sum of variances and sum of ranges disparity analyses, mosasaurids demonstrate higher mean disparity than cetaceans (Fig. 3A, Supplementary Fig. 1). Furthermore, in the sum of ranges analysis, both individual mosasaurid subclades (Russellosaurina and Mosasaurinae) exhibit higher disparity than the cetacean subclades (Fig. 3B). However, when sum of variance is used, the unusual mysticete *Janjucetus hunderi* drives a higher disparity result in this subclade (Fig. 3A, Supplementary Fig. 2).

Unlike their mosasaurid counterparts, the earliest fully aquatic cetaceans (basilosaurid "archaeocetes") had large skulls with extensive areas of temporal musculature and robust teeth (low crown aspect ratio) and plot close to the megapredatory mosasaurids *Mosasaurus* and *Tylosaurus* (Fig. 2B, Supplementary Fig. 3). All "archaeocetes" plot in a similar region of ecomorphospace (Fig. 2B) and show low ecomorphological disparity when compared with both mosasaurid clades and more derived cetaceans (Fig. 3B). Variation in this group is spread along an axis describing postorbital robusticity, with the basilosaurid *Basilosaurus* exhibiting a deep postorbital skull and large, robust anterior dentition compared with the more flattened,
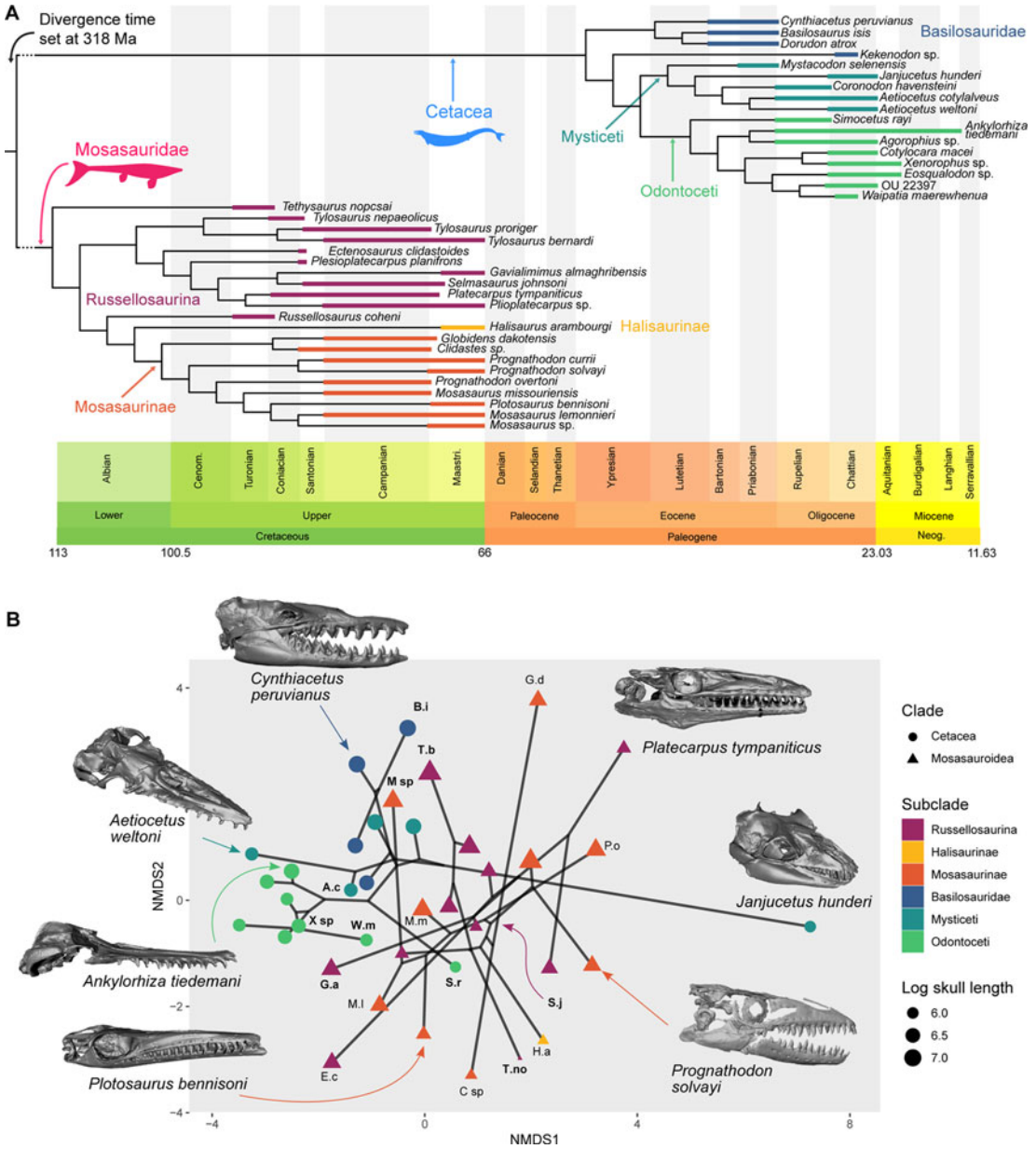
FIGURE 2.   A, Phylogenetic supertree of all taxa used in analyses, based on Martínez-Cáceres et al. 2017 (cetaceans) and Strong et al. 2020 (mosasaurids). B, Craniodental phylo-ecomorphospace occupation by mosasaurids and early cetaceans (based on nonmetric multidimensional scaling [NMDS] axes). Taxon names in bold are included in the convergence tests. Taxon abbreviations: A.c, *Aetiocetus cotylalveus*, B.i, *Basilosaurus isis*; C sp, *Clidastes* sp., E.c, *Ectenosaurus clidastoides*; G.a, *Gavialimimus almaghribensis*; G.d, *Globidens dakotensis*; H.a, *Halisaurus arambourgi*; M.l, *Mosasaurus lemonnieri*; M.m, *Mosasaurus missouriensis*; M sp, *Mosasaurus* sp.; P.o, *Prognathodon overtoni*; S.j, *Selmasaurus johnsoni*, S.r, *Simocetus rayi*; T.b, *Tylosaurus bernardi*; T.no, *Tethysaurus nopcsai*; W.m, *Waipatia maerewhenua*, X sp, *Xenorophus* sp. Point sizes scaled to log skull length.

shallow-snouted cranium of *Kekenodon* (Supplementary Fig. 4). Oligocene toothed mysticetes are more disparate than both odontocetes and basilosaurids (Fig. 3B), which is reflected in both the results of the disparity analysis as well as their spread across the

TABLE 3. Results of Stayton convergence tests, reported to four decimal places. M, Mosasauridae; C, Cetacea; Mos, Mosasaurina; Rus, Russellosaurina; Odo, Odontoceti; Mys, Mysticeti. PCo, principal coordinates. Asterisks in *p*-value column indicate significance at: *$p < 0.05$; **$p < 0.01$; ***$p < 0.001$.

Taxon pair	PCo axes	C1	*p*-value
Janjucetus hunderi (C)–	PCo1-2	0	0.9990
Prognathodon solvayi (M)	All	0	0.9990
Basilosaurus isis (C)–	PCo1-2	0.6137	0.0150*
Tylosaurus bernardi (M)	All	0.2936	0***
Mosasaurus sp. (M)–	PCo1-2	0.9202	0.0010***
Cynthiacetus peruvianus (C)	All	0.4207	0***
Tethysaurus nopcsai (Rus)–*Plotosaurus*	PCo1-2	0.0180	0.5205
bennisoni (Plo)	All	0.3131	0.0180*
Waipatia maerewhenua (C)–	PCo1-2	0.8383	0.0070**
Gavialimimus almaghribensis (M)	All	0.5713	0***
Aetiocetus cotylalveus (Mys)–	PCo1-2	0.8571	0.0070**
Xenorophus sp. (Odo)	All	0.2073	0.0330*
Simocetus rayi (C)–	PCo1-2	0.7747	0.0040**
Selmasaurus johnsoni (M)	All	0.1116	0.1079

ecomorphospace (Figs. 2B, 3B). However, as already mentioned, this high disparity is primarily driven by the presence of *J. hunderi* (Supplementary Fig. 2). Archaic mysticetes (*Mystacodon selenensis* and *Coronodon havensteini*) plot close to basilosaurids, whereas more crownward forms (aetiocetids) occupy a region of ecomorphospace characterized by long, thin snouts and smaller, narrower teeth. The mammalodontid *J. hunderi* consistently stands apart from the other cetaceans; it has a large relative temporal fenestra size, with high ratios for snout width, snout depth, and orbit diameter (Supplementary Fig. 5) and plots as an outlier to both cetacean and mosasaurid ecomorphospace occupation (Fig. 2B). Early odontocetes evolved a suite of features associated with more longirostrine snouts and smaller teeth, indicating a somewhat more constricted ecomorphospace occupation by early odontocetes and aetiocetes. The basal odontocete *Simocetus rayi* plots within the center of mosasaurid ecomorphospace, despite notable morphological differences between *Simocetus* and the majority of mosasaurids.

With the exception of the toothed mysticete *J. hunderi* (see below), cetaceans in general have shallower snouts, smaller orbits, and more variably sized—and often larger—temporal fenestrae (Supplementary Figs. 5, 6) than mosasaurids. Furthermore, cetaceans show a wider range of adductor mechanical advantage, including the species with the lowest (*Aetiocetus weltoni*) and highest (*J. hunderi*)

values (Supplementary Figs. 5, 6). The size range for mosasaurids and cetaceans (using both metrics) is similar, with the cetacean distribution indicating larger skulls overall than mosasaurids (Fig. 3C,D). Only two pairs of functional traits are significantly correlated across both mosasaurs and cetaceans: snout depth to temporal fenestra length (mosasaur $R = 0.67$; cetacean $R = 0.84$) and snout depth to snout width (mosasaur $R = 0.80$; cetacean $R = 0.75$) (Supplementary Figs. 5, 6). Some of the other correlated traits in cetaceans are likely due to one outlying taxon (*J. hunderi*; Supplementary Fig. 5). Neither the NMDS nor the PCoA plots clearly distinguish long- from robust-snouted species (Fig. 2, Supplementary Fig. 7). Putative apex predators, inferred as active hunters of large vertebrate prey, plot at higher values on both axes irrespective of the ordination method (e.g., the mosasaurids *Tylosaurus bernardi* and *Prognathodon overtoni*, and the cetacean *Basilosaurus isis*). There is no obvious association between locomotion guild and either skull ecomorphology or dietary class (Supplementary Figs. 3, 8). However, it should be noted that both dietary class and locomotion guild have a high percentage (around 65%) of missing data (Supplementary Material).

Convergence Tests.—Statistical analyses identify a number of different taxa as convergent in their skull ecomorphology, albeit at different levels (Table 3). Three mosasaurid–cetacean pairs were statistically convergent for both sets of PCoA axes tested: *Gavialimimus almaghribensis* versus *Waipatia maerewhenua*; *T. bernardi* versus
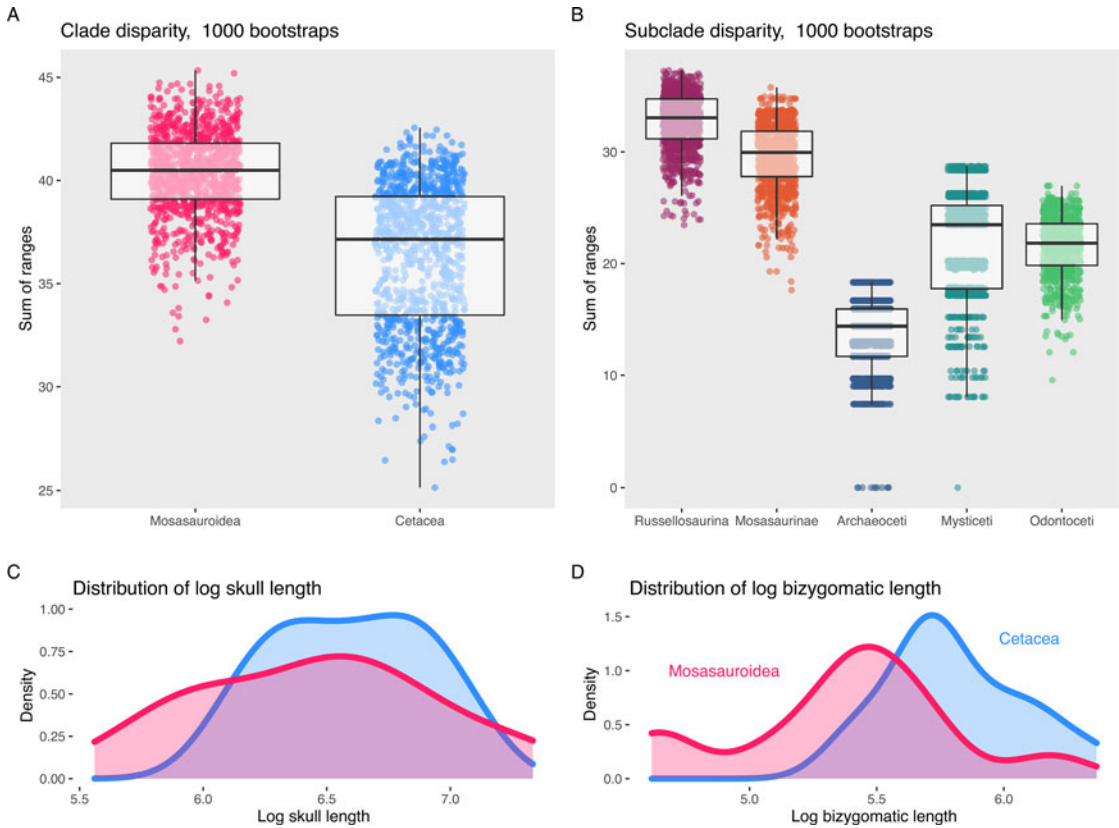
FIGURE 3.   Comparisons of ecomorphological disparity (A) between mosasaurids and early cetaceans and (B) between sub-clades. Sum of ranges metric, 1000 bootstrap replications. Histograms showing size distribution among the two clades using two metrics: (C) log skull length and (D) log bizygomatic width.

B. isis; and *Mosasaurus* sp. (IRSNB R 12) versus *Cynthiacetus peruvianus*. Convergence was also recovered for the mysticete–odontocete pair *Aetiocetus cotylalveus* versus *Xenorophus* sp. (Table 3). Evidence for convergence between other selected pairs was less strongly supported (e.g., *Tethysaurus nopcsai* versus *Plotosaurus bennisoni*; *S. rayi* vs. *Selmasaurus johnsoni*) or absent entirely (*J. hunderi* vs. *Prognathodon solvayi*). When the divergence date was set to the minimum branch length, the exact values of the C1 metric and associated *p*-values change slightly but the same pairs remain significant (Supplementary Table 3).

Discussion

Differences in Evolutionary Trajectory.—Early mosasaurids and archaeocete cetaceans occupy clearly distinct regions of the ecomorphospace,

possibly reflecting their different terrestrial ancestries. Little is known about the ecology of semiaquatic mosasauroids ("aigialosaurs"), with most research instead focusing on their phylogenetic relationships to other squamates (Carroll and Debraga 1992). However, these were small reptiles with skulls and teeth comparable to those of early mosasaurids and a probable diet of small prey (Carroll and Debraga 1992; Bardet et al. 2008; Cross et al. 2022). By contrast, semiaquatic archaeocetes not included in this study (e.g., *Protocetus*) were relatively large and powerful, with a diet that likely consisted of a wide variety of prey types and sizes (Fahlke et al. 2013). The difference in ecomorphospace occupation between basilosaurids and early mosasaurids could also reflect available niche space. In the aftermath of the K/Pg mass extinction, early cetaceans likely faced relatively little

competition other than selachians (Lindberg and Pyenson 2006). This was not the case during the Cenomanian–Turonian radiation of mosasauroids, which had to navigate coexistence with other marine reptiles, including large platypterygiine ichthyosaurians, both long- and short-necked plesiosaurians, sharks, and large teleosts (Bardet 1994; Fischer 2016; Reeves et al. 2021; Cross et al. 2022). It is possible that marine ecosystem turnover and the demise of ichthyosaurs at the end of the Cenomanian allowed mosasaurids to diversify and occupy higher trophic levels (Bardet et al. 2008; Cross et al. 2022).

Mosasaurids and cetaceans both radiated during times of high marine productivity (Polcyn et al. 2014; Pyenson et al. 2014), but did so at different stages in their respective evolutionary histories. Our results suggest that mosasaurids radiated in skull ecomorphology soon after becoming fully aquatic; however, it should be noted that the fossil record of these early forms is poor (Cross et al. 2022). This is in contrast to basilosaurid cetaceans, whose skulls remained comparatively ecomorphologically conserved until the origin of neocetes during the latest Eocene (Boessenecker et al. 2017b; Coombs et al. 2022; Fig. 2B). The ecomorphological evolution of mosasaurids lacks an obvious pattern. In several cases, later and highly derived forms plot in proximity to less-derived predecessors; one striking example of this is the mosasaurine *Plotosaurus bennisoni*, which occupies a region of cranial ecomorphospace similar to that of more basal mosasaurids (Fig. 2) such as *Clidastes* and *Tethysaurus* (Fig. 2B, Supplementary Fig. 4), despite its highly derived akinetic skull and postcranial anatomy (Lindgren et al. 2007; LeBlanc et al. 2013). In fact, our analysis recovered *Plotosaurus* as statistically convergent with one of the oldest mosasaurid species in the analysis, the russellosaurine *Tethysaurus nopcsai* (Table 3), demonstrating that for the craniodental characteristics investigated in this study, both early (basal) and late (derived) mosasaurids from a wide range of phylogenetic clades may have adopted similar functional roles, albeit likely at different scales given the discrepancy in body sizes between the taxa (Fig. 2). At least six mosasaurid taxa occupy a region of low NMDS 2 values, with

many of these species exhibiting elongate rostra and narrow dentition (e.g., *Ectenosaurus*, *Plotosaurus*, *Tethysaurus*) often associated with rapid jaw adduction and fast-prey capture. Although specimen selection may have influenced overall values and placement in ecomorphospace (e.g., *P. bennisoni* UCMP 32778 is possibly a juvenile; LeBlanc et al. 2013), the size-independent nature of most of the functional characteristics used precludes large differences to be expected from ontogeny, and we find no evidence for severe ontogenetic allometry in mosasaurids in the literature. Rather than radiating out from one common source and not reverting, mosasaurids from different times and phylogenetic clades are recovered in similar regions of ecomorphospace, indicating a recurring longirostrine ecomorphology transcendent of phylogenetic relatedness (Fig. 2B). Overall, mosasaurids do not follow a clear trajectory within ecomorphospace occupation in relation to phylogeny or temporal occurrence, but rather occupy a range of ecomorphospace indicative of widespread niche partitioning within and between clades (Schulp et al. 2013).

The trajectory of early cetacean skull ecomorphological evolution is much easier to discern than for mosasaurids. Basilosaurids all occupy a similar region of ecomorphospace (Fig. 2B, high NMDS 2). The earliest mysticetes in the study (*Mystacodon* and *Coronodon*) plot near basilosaurid ecomorphospace; subsequently, both mysticetes and odontocetes evolved along similar (but nonidentical) trajectories toward shallower, longer snouts with smaller teeth. We interpret these changes as adaptations to feeding on smaller prey (reducing the necessity for high bending resistance in the snout and mandible), as also reflected in the gradual emergence of simplified teeth and the attendant need to swallow prey whole (Peredo et al. 2018). Innovations in feeding ecology may have been a major driver of neocete (mysticetes + odontocetes) diversification (Marx and Fordyce 2015; Boessenecker et al. 2017b). Some highly distinctive taxa like the odontocete *Inermorostrum* and the toothed mysticete *Mammalodon* were too incomplete to include in our analysis, and early toothless mysticetes were not considered ecologically

comparable to mosasaurids; the inclusion of these taxa would likely have increased the ecomorphological disparity of Oligocene neocetes even more so than is recovered with the taxa sampled here (Figs. 2B, 3).

Some cetaceans diverge significantly from the trajectories seen in the rest of the clade. For example, the earliest odontocete *Simocetus rayi* plots among the mosasaurids and is at least slightly convergent with the small plioplatecarpine mosasaurid *Selmasaurus johnsoni* (Table 3). This result may be spurious, as *Simocetus* has a highly unusual skull shape—including edentulous premaxillae and a ventrally deflected rostrum (Fordyce 2002)—not captured by our functional trait measurements. These and other features have led to *Simocetus* being interpreted as a benthic suction feeder, a lifestyle seemingly never adopted by mosasaurids. Any similarities between the two, such as a relatively short and deep snout, are thus likely superficial rather than functional in nature.

The same may be true for the unusual Oligocene toothed mysticete *Janjucetus hunderi*, whose deep, blunt snout and large eyes may reflect a route to a megapredatory ecomorphology quite removed from that of mosasaurids (e.g., *Mosasaurus* spp. and *Prognathodon currii*); these morphological features may also be directly involved in suction feeding (Fitzgerald 2010, 2012; Young et al. 2012). This taxon is an outlier in our analyses, and despite plotting closest to the mosasaurid *Prognathodon solvayi*, the two are not significantly convergent. *Janjucetus hunderi* has the largest relative temporal fenestra size and anterior mechanical advantage of all the species in this study, suggesting a slow and powerful bite, whereas *P. solvayi* has values that are comparatively unremarkable compared with other taxa in the analysis. *Janjucetus* has been compared with various other secondarily aquatic tetrapods, including the plesiosaur *Rhomaleosaurus* (Fitzgerald 2006), the metriorhynchid *Dakosaurus* (Young et al. 2012), and the pinniped *Hydrurga* (Fitzgerald 2006). The deep snouts of all these taxa are well adapted for resisting torsional stress during grip and tear feeding (Taylor 1992; Fitzgerald 2006; Young et al. 2012), and their size range suggests that this feeding

style was possible for both apex and lower-level megapredators. The stark contrast between the stout, brevirostrine snouts of mammalodontid odontocetes (such as *Janjucetus*) compared with the elongate, latirostrine crania of both aetiocetid mysticetes (e.g., *Aetiocetus*) and many Oligocene odontocetes (e.g., *Xenorophus*) indicates a clear divergence in ecomorphological trajectory in Oligocene cetaceans. Interestingly, occupation of ecomorphospace by all three of these groups is not shared with any group of mosasaurids.

One of the more surprising results of our analysis was the apparent decoupling of swimming ability and cranial ecomorphology, with sub-carangiform and carangiform species plotting broadly with their anguilliform ancestors. Despite the limitations of our postcranial dataset, this result is consistent with other studies indicating distinct evolutionary pressures on craniodental and postcranial regions—for example, in short-necked plesiosaurs (Fischer et al. 2020) and ichthyosaurs (Gutarra et al. 2019).

Convergence, Heritage, and Context.—Despite being statistically significant, the convergence recovered between three mosasaurid-cetacean pairs (*Basilosaurus isis* vs. *Tylosaurus bernardi*, *Cynthiacetus peruvianus* vs. *Mosasaurus* sp. (IRSNB R 12), and *Waipatia maerewhenua* vs. *Gavialimimus almaghribensis*) is not reflected in a complete overlap of ecomorphospace occupation between the two clades. They are thus examples of incomplete convergence, wherein taxa are ecomorphologically similar—for example, the presence of a robust skull and elongate snout in *B. isis*/*T. bernardi* and *C. peruvianus*/*Mosasaurus* sp.—yet exhibit unique morphological traits (Grossnickle et al. 2020; Watanabe et al. 2021). The latter may be unique adaptations, such as the predental rostrum of *T. bernardi* (Jiménez-Huidobro and Caldwell 2016) and the distinctive prismatic cutting edges on the teeth of *Mosasaurus* (Lingham-Soliar 1995), or ancestral constraints, such as pterygoid teeth and cranial kinesis in mosasaurids (LeBlanc et al. 2013) and heterodont teeth and the mammalian jaw joint in early cetaceans (Uhen 2018).

One previous study interpreted *Basilosaurus* as an "Elvis taxon" that filled a niche vacated

by megapredatory mosasaurids at the K/Pg boundary (Gallagher 2014). The term "Elvis taxon" was erected to describe a phenomenon seen during postextinction recovery among invertebrate communities whereby a morphology reappears long after it was thought to have become extinct (Erwin and Droser 1993). The original extinct species is replaced by a new, unrelated form that is morphologically indistinguishable from its predecessor (Erwin and Droser 1993). This situation clearly does not apply to *B. isis* and *T. bernardi*, which are not morphologically identical. In addition to these ecomorphological differences, substantial changes took place in oceanic ecosystems at the K/Pg boundary and in the 15 Myr of subsequent recovery before the first semiaquatic archaeocetes evolved (Thewissen et al. 2009). Late Cretaceous oceans were particularly hot and deep and sometimes poorly oxygenated (Skelton et al. 2003), whereas the late Eocene oceans were cooler and punctuated at the Eocene–Oligocene boundary by the onset of Antarctic glaciation and the precursor of the Antarctic Circumpolar Current (Marx and Fordyce 2015). Rather than filling a specifically mosasaurid-shaped hole, *B. isis* emerged in the context of an ecosystem that had recovered from the bottom up and lacked any large secondarily aquatic tetrapod predators. Instead of one impersonating the other, *B. isis* and *T. bernardi* might be better understood as large open-ocean megapredators with similar craniodental proportions, reflecting the constraints of their shared ecological niche.

Convergence between the longirostrine mosasaurid *G. almaghribensis* and the odontocete *W. maerewhenua* (Table 3) also highlights the repeated evolution of longirostrine (putatively piscivorous) ecomorphologies in marine amniotes. Longirostry is thought to increase hydrodynamic efficiency during sweep feeding on small, fast prey (McCurry et al. 2017a; Strong et al. 2020), and longirostrine species have jaws that are biomechanically adapted to open swiftly and capture prey (Anderson et al. 2011). Our results suggest that early odontocetes were able to explore longirostry to a greater extent than mosasaurids. Whereas *G. almaghribensis* is one of the most longirostrine mosasaurids in this study, *W.*

maerewhenua has a shorter rostrum than several other early odontocetes and may have been a ram feeder (Tanaka and Fordyce 2017). Longirostry in early odontocetes perhaps evolved in tandem with both cranial telescoping and echolocation (Geisler et al. 2014; Boessenecker et al. 2017b). While we cannot know how mosasaurids would have evolved had they survived the K/Pg mass extinction, it is clear that later odontocetes evolved extremely elongate rostra (Lambert and Goolaerts 2021).

Our results add to increasing evidence that incomplete convergence is more common in the natural world than previously realized (Meloro et al. 2015; Grossnickle et al. 2020; Watanabe et al. 2021; Alfieri et al. 2022) and suggest that the textbook convergence in marine tetrapods may be superficial and likely restricted to general body shape (Motani 2002). When one focuses in on the details of craniodental architecture, strong ecomorphological convergence appears rare, especially when analyzing distant clades that colonized marine niches in widely distinct biosphere contexts, such as mosasaurids and early cetaceans. Strong ecomorphological convergence has been theorized to occur when considering a specific, restricted niche with a single optimal morphology (Alfieri et al. 2022); this has been observed in short-necked plesiosaurs, which have an adaptive landscape defined by "peaks" of optimal morphology (Fischer et al. 2020). However, incomplete convergence may result in an adaptive landscape better described as a "slope," where groups show similar or parallel trajectories in ecomorphological evolution that are offset by their ancestral heritage (Grossnickle et al. 2020; Alfieri et al. 2022). Our results fit this pattern, with no clear optimal peaks of ecomorphology and trajectories that appear to be strongly influenced by intrinsic phylogenetic constraints. We posit that extrinsic environmental influences, such as differences in ocean temperature and oxygenation between the Late Cretaceous and Eocene–Oligocene (Skelton et al. 2003; Marx and Fordyce 2015), as well as available ecological niche space in the pelagic ecosystem, were of importance. These distinct contexts likely combined with phyletic heritage and historical contingency to limit marine tetrapod

convergence. While we did not consider convergence in postcranial anatomy during this study, it is likely that this would show a similar trend—broad similarities in axial or appendicular morphology that are limited by constraint inherited from mammalian or reptilian ancestors (e.g., dorsoventral vs. lateral axial movement).

Incomplete convergence can also occur as a result of multiple morphologies performing the same purpose, a "many-to-one" relationship between form and function (Zelditch et al. 2017). This has been seen in a number of terrestrial groups, including pack-hunting carnivorans (Meloro et al. 2015), gliding mammals (Grossnickle et al. 2020), and slow arboreal xenarthrans (Alfieri et al. 2022). Modern (and presumably also extinct) marine raptorial predators are usually opportunistic and often overlap in prey choice and capture methods (Hocking et al. 2017). Our study highlights the complicated relationship between form and function in these animals, which may best be described as "many-to-many" (Zelditch et al. 2017).

Conclusions

Despite their superficial similarities, mosasaurids and early cetaceans show different evolutionary trajectories in skull ecomorphology. The earliest mosasaurids were small, low-level predators that rapidly radiated into a range of different ecomorphologies and inferred niches. By contrast, early fully aquatic cetaceans were likely all megapredatory and show a general evolutionary trend toward adaptations for smaller prey. The evolutionary pathways in these groups are strongly influenced by intrinsic phylogenetic constraints as well as extrinsic environmental influences.

We found several examples of convergence in skull ecomorphology between megapredatory forms, but also between longirostrine forms. Despite numerous shared features, convergence is generally incomplete and neither overrides ancestral constraints nor precludes the presence of unique adaptations in certain species. Our results suggest that qualitative assessment of marine tetrapod convergence is too superficial and can overlook the more nuanced differences in ecomorphology between different secondarily aquatic tetrapod radiations.

Data Availability Statement

Data available from the Dryad Digital Repository: https://doi.org/10.5061/dryad.0rxwdbs3m.

Literature Cited

Alfieri, F., L. Botton-Divet, J. A. Nyakatura, and E. Amson. 2022. Integrative approach uncovers new patterns of ecomorphological convergence in slow arboreal xenarthrans. Journal of Mammalian Evolution 29:283–312.

Anderson, P. S. L., M. Friedman, M. D. Brazeau, and E. J. Rayfield. 2011. Initial radiation of jaws demonstrated stability despite faunal and environmental change. Nature 476:206–209.

Bapst, D. W. 2012. paleotree: an R package for paleontological and phylogenetic analyses of evolution. Methods in Ecology and Evolution 3:803–807.

Bardet, N. 1994. Extinction events among Mesozoic marine reptiles. Historical Biology 7:313–324.

Bardet, N., A. Houssaye, J. C. Rage, and X. Pereda Suberbiola. 2008. The Cenomanian–Turonian (late Cretaceous) radiation of marine squamates (Reptilia): the role of the Mediterranean Tethys. Bulletin de la Societe Geologique de France 179:605–622.

Boessenecker, R. W., E. Ahmed, and J. H. Geisler. 2017a. New records of the dolphin Albertocetus meffordorum (Odontoceti: Xenorophidae) from the lower Oligocene of South Carolina: encephalization, sensory anatomy, postcranial morphology, and ontogeny of early odontocetes. PLoS ONE 12:e0186476.

Boessenecker, R. W., D. Fraser, M. Churchill, and J. H. Geisler. 2017b. A toothless dwarf dolphin (Odontoceti: Xenorophidae) points to explosive feeding diversification of modern whales (Neoceti). Proceedings of the Royal Society of London B 284:20170531.

Boessenecker, R. W., M. Churchill, E. A. Buchholtz, B. L. Beatty, and J. H. Geisler. 2020. Convergent evolution of swimming adaptations in modern whales revealed by a large macrophagous dolphin from the Oligocene of South Carolina. Current Biology 30:3267–3273.

Brocklehurst, N., D. P. Ford, and R. B. J. Benson. 2022. Early origins of divergent patterns of morphological evolution on the mammal and reptile stem-lineages. Systematic Biology. doi: 10.1093/sysbio/syac020.

Buchholtz, E. A. 2001. Vertebral osteology and swimming style in living and fossil whales (Order: Cetacea). Journal of Zoology 253:175–190.

Buono, M. R., R. Fordyce, F. G. Marx, M. Fernandez, and M. A. Reguero. 2019. Eocene Antarctica: a window into the earliest origins of modern whales. Advances in Polar Science 30:1–10.

Carroll, R. L., and M. Debraga. 1992. Aigialosaurs: mid-Cretaceous varanoid lizards. Journal of Vertebrate Paleontology 12:66–86.

Christiansen, P., and N. Bonde. 2002. A new species of gigantic mosasaur from the Late Cretaceous of Israel. Journal of Vertebrate Paleontology 22:629–644.

Clementz, M. T., R. E. Fordyce, S. L. Peek, and D. L. Fox. 2014. Ancient marine isoscapes and isotopic evidence of bulk-feeding by Oligocene cetaceans. Palaeogeography, Palaeoclimatology, Palaeoecology 400:28–40.

Coombs, E. J., R. N. Felice, J. Clavel, T. Park, R. F. Bennion, M. Churchill, J. H. Geisler, B. Beatty, and A. Goswami. 2022. The tempo of cetacean cranial evolution. Current Biology 32:2233–2247.e4.

Coste, A., R. E. Fordyce, and C. Loch. 2018. Form, function, and phylogeny in Late Oligocene tusked dolphins from New Zealand. Fifth International Palaeontological Congress, Paris, France, 9–13 July 2018.

Cross, S. R. R., B. C. Moon, T. L. Stubbs, E. J. Rayfield, and M. J. Benton. 2022. Climate, competition, and the rise of mosasauroid ecomorphological disparity. Palaeontology 65:1–24.

Erwin, D. H., and M. L. Droser. 1993. Elvis taxa. Palaios 8:623–624.

Everhart, M. J. 2005. Rapid evolution , diversification and distribution of mosasaurs (Reptilia; Squamata) prior to the K-T boundary. Tate 2005: 11th Annual Symposium in Paleontology and Geology, Casper, Wyo., pp. 16–27.

Fahlke, J. M., K. A. Bastl, G. M. Semprebon, and P. D. Gingerich. 2013. Paleoecology of archaeocete whales throughout the Eocene: dietary adaptations revealed by microwear analysis. Palaeogeography, Palaeoclimatology, Palaeoecology 386:690–701.

Fischer, V. 2016. Taxonomy of Platypterygius campylodon and the diversity of the last ichthyosaurs. PeerJ 4:e2604.

Fischer, V., R. B. J. Benson, N. G. Zverkov, L. C. Soul, M. S. Arkhangelsky, O. Lambert, I. M. Stenshin, G. N. Uspensky, and P. S. Druckenmiller. 2017. Plasticity and convergence in the evolution of short-necked plesiosaurs. Current Biology 27:1667–1676.

Fischer, V., J. A. MacLaren, L. C. Soul, R. F. Bennion, P. S. Druckenmiller, and R. B. J. Benson. 2020. The macroevolutionary landscape of short-necked plesiosaurians. Scientific Reports 10:1–12.

Fish, F. E. 2001. A mechanism for evolutionary transition in swimming mode by mammals. Pp. 261–287 in J.-M. Mazin and V. de Buffrénil, eds. Secondary adaptations of tetrapods to life in water. Verlag Dr. Friedrich Pfeil, Munich, Germany.

Fitzgerald, E. M. G. 2006. A bizarre new toothed mysticete (Cetacea) from Australia and the early evolution of baleen whales. Proceedings of the Royal Society of London B 273:2955–2963.

Fitzgerald, E. M. G. 2010. The morphology and systematics of Mammalodon colliveri (Cetacea: Mysticeti), a toothed mysticete from the Oligocene of Australia. Zoological Journal of the Linnean Society 158:367–476.

Fitzgerald, E. M. G. 2012. Archaeocete-like jaws in a baleen whale. Biology Letters 8:94–96.

Fordyce, R. E. 2002. Simocetus rayi (Odontoceti: Simocetidae, New Family): a bizarre new archaic Oligocene dolphin from the eastern North Pacific. Smithsonian Contributions to Paleobiology 93:185–222.

Gallagher, W. B. 2014. Greensand mosasaurs of New Jersey and the Cretaceous–Paleogene transition of marine vertebrates. Geologie en Mijnbouw/Netherlands Journal of Geosciences 94:87–91.

Geisler, J. H., M. W. Colbert, and J. L. Carew. 2014. A new fossil species supports an early origin for toothed whale echolocation. Nature 508:383–386.

Geisler, J. H., R. W. Boessenecker, M. Brown, and B. L. Beatty. 2017. The origin of filter feeding in whales. Current Biology 27:2036–2042.e2.

Grossnickle, D. M., M. Chen, J. G. A. Wauer, S. K. Pevsner, L. N. Weaver, Q. J. Meng, D. Liu, Y. G. Zhang, and Z. X. Luo. 2020. Incomplete convergence of gliding mammal skeletons. Evolution 74:2662–2680.

Guillerme, T. 2018. dispRity: a modular R package for measuring disparity. Methods in Ecology and Evolution 9:1755–1763.

Gutarra, S., and I. A. Rahman. 2022. The locomotion of extinct secondarily aquatic tetrapods. Biological Reviews 97:67–98.

Gutarra, S., B. C. Moon, I. A. Rahman, C. Palmer, S. Lautenschlager, A. J. Brimacombe, and M. J. Benton. 2019. Effects of body plan evolution on the hydrodynamic drag and energy requirements of swimming in ichthyosaurs. Proceedings of the Royal Society of London B 286:20182786.

Hocking, D. P., F. G. Marx, T. Park, E. M. G. Fitzgerald, and A. R. Evans. 2017. A behavioural framework for the evolution of feeding in predatory aquatic mammals. Proceedings of the Royal Society of London B 284:20162750.

Jimenéz-Huidobro, P., and M. W. Caldwell. 2016. Reassessment and reassignment of the early Maastrichtian mosasaur Hainosaurus bernardi Dollo, 1885, to Tylosaurus Marsh, 1872. Journal of Vertebrate Paleontology 36:e1096275.

Jiménez-Huidobro, P., T. R. Simões, and M. W. Caldwell. 2017. Mosasauroids from Gondwanan continents. Journal of Herpetology 51:355–364.

Kelley, N. P., and R. Motani. 2015. Trophic convergence drives morphological convergence in marine tetrapods. Biology Letters 11:20140709.

Kelley, N. P., and N. D. Pyenson. 2015. Evolutionary innovation and ecology in marine tetrapods from the Triassic to the Anthropocene. Science 348:aaa3716.

Konishi, T., D. Brinkman, J. A. Massare, and M. W. Caldwell. 2011. New exceptional specimens of *Prognathodon overtoni* (Squamata, Mosasauridae) from the upper Campanian of Alberta, Canada, and the systematics and ecology of the genus. Journal of Vertebrate Paleontology 31:1026–1046.

Lambert, O., and S. Goolaerts. 2021. Late Miocene survival of a hyper-longirostrine dolphin and the Neogene to Recent evolution of rostrum proportions among odontocetes. Journal of Mammalian Evolution 29:99–111.

Lambert, O., M. Martínez-Cáceres, G. Bianucci, C. Di Celma, R. Salas-Gismondi, E. Steurbaut, M. Urbina, and C. de Muizon. 2017. Earliest mysticete from the Late Eocene of Peru sheds new light on the origin of baleen whales. Current Biology 7:229–264.

LeBlanc, A. R. H., M. W. Caldwell, and J. Lindgren. 2013. Aquatic adaptation, cranial kinesis, and the skull of the mosasaurine mosasaur *Plotosaurus bennisoni*. Journal of Vertebrate Paleontology 33:349–362.

Lindberg, D. R., and N. D. Pyenson. 2006. Evolutionary patterns in Cetacea fishing up prey size through deep time. Pp. 68–82 in J. A. Estes, D. P. Demaster, D. F. Doak, T. M. Williams, and R. L. Brownell, eds. Whales, Whaling, and Ocean Ecosystems. 1st ed. University of California Press, Berkeley.

Lindgren, J., J. W. M. Jagt, and M. W. Caldwell. 2007. A fishy mosasaur: the axial skeleton of *Plotosaurus* (Reptilia, Squamata) reassessed. Lethaia 40:153–160.

Lindgren, J., M. W. Caldwell, T. Konishi, and L. M. Chiappe. 2010. Convergent evolution in aquatic tetrapods: insights from an exceptional fossil mosasaur. PLoS ONE 5:1–10.

Lindgren, J., M. J. Polcyn, and B. A. Young. 2011. Landlubbers to leviathans: evolution of swimming in mosasaurine mosasaurs. Paleobiology 37:445–469.

Lingham-Soliar, T. 1995. Anatomy and functional morphology of the largest marine reptile known, *Mosasaurus hoffmanni* (Mosasauridae, Reptilia) from the Upper Cretaceous, Upper Maastrichtian of the Netherlands. Philosophical Transactions of the Royal Society of London B 347:155–180.

MacLaren, J. A., P. S. L. Anderson, P. M. Barrett, and E. J. Rayfield. 2017. Herbivorous dinosaur jaw disparity and its relationship to extrinsic evolutionary drivers. Paleobiology 43:15–33.

MacLaren, J. A., R. F. Bennion, N. Bardet, and V. Fischer. 2022. Global ecomorphological restructuring of dominant marine reptiles prior to the K/Pg mass extinction. Proceedings of Royal Society of London B 289:20220585.

Martínez-Cáceres, M., O. Lambert, and C. de Muizon. 2017. The anatomy and phylogenetic affinities of *Cynthiacetus peruvianus*, a large *Dorudon*-like basilosaurid (Cetacea, Mammalia) from the late Eocene of Peru. Geodiversitas 7207:7–163.

Marx, F. G., and R. E. Fordyce. 2015. Baleen boom and bust: a synthesis of mysticete phylogeny, diversity and disparity. Royal Society Open Science 2:140434.

McCurry, M. R., A. R. Evans, E. M. G. Fitzgerald, J. W. Adams, P. D. Clausen, and C. R. McHenry. 2017a. The remarkable convergence of skull shape in crocodilians and toothed whales. Proceedings of Royal Society of London B 284:9–11.

McCurry, M. R., E. M. G. Fitzgerald, A. R. Evans, J. W. Adams, and C. R. McHenry. 2017b. Skull shape reflects prey size niche in toothed whales. Biological Journal of the Linnean Society 121:936–946.

Meloro, C., M. Clauss, and P. Raia. 2015. Ecomorphology of Carnivora challenges convergent evolution. Organisms Diversity and Evolution 15:711–720.

Motani, R. 2002. Swimming speed estimation of extinct marine reptiles: energetic approach revisited. Paleobiology 28:251–262.

Motani, R., X.-H. Chen, D.-Y. Jiang, L. Cheng, A. Tintori, and O. Rieppel. 2015. Lunge feeding in early marine reptiles and fast evolution of marine tetrapod feeding guilds. Scientific Reports 5:8900.

Muizon, C. de. 1991. A new Ziphiidae (Cetacea) from the Early Miocene of Washington State (USA) and phylogenetic analysis of the major groups of odontocetes. Bulletin du Muséum national d'Histoire naturelle, Paris, 4e série, section C 12:279–326.

Oksanen, J., R. Kindt, P. Legendre, B. O'Hara, G. L. Simpson, P. Solymos, M. H. H. Stevens, and H. Wagner.. 2007. The vegan package. Community ecology package 10:719. https://CRAN.R-project.org/package=vegan, accessed 29 April 2022.

Paradis, E., J. Claude, and K. Strimmer. 2004. APE: analyses of phylogenetics and evolution in R language. Bioinformatics 20:289–290.

Pauly, D., A. W. Trites, E. Capuli, and V. Christensen. 1998. Diet composition and trophic levels of marine mammals. ICES Journal of Marine Science 55:467–481.

Peredo, C. M., J. S. Peredo, and N. D. Pyenson. 2018. Convergence on dental simplification in the evolution of whales. Paleobiology 44:434–443.

Polcyn, M. J., and G. L. Bell. 2005. *Russellosaurus coheni* n. gen., n. sp., a 92 million-year-old mosasaur from Texas (USA), and the definition of the parafamily Russellosaurina. Netherlands Journal of Geosciences 84:321–333.

Polcyn, M. J., J. Lindgren, N. Bardet, D. Cornelissen, L. Verding, and A. S. Schulp. 2012. Description of new specimens of *Halisaurus arambourgi* Bardet & Pereda Soberbiola, 2005 and the relationships of Halisaurinae. Bulletin de la Societe Geologique de France 183:123–136.

Polcyn, M. J., L. L. Jacobs, A. Araújo, A. S. Schulp, and O. Mateus. 2014. Physical drivers of mosasaur evolution. Palaeogeography, Palaeoclimatology, Palaeoecology 400:17–27.

Pyenson, N. D., and S. N. Sponberg. 2011. Reconstructing body size in extinct crown Cetacea (Neoceti) using allometry, phylogenetic methods and tests from the fossil record. Journal of Mammalian Evolution 18:269–288.

Pyenson, N. D., N. P. Kelley, and J. F. Parham. 2014. Marine tetrapod macroevolution: physical and biological drivers on 250Ma of invasions and evolution in ocean ecosystems. Palaeogeography, Palaeoclimatology, Palaeoecology 400:1–8.

R Core Team. 2021. R: a language and environment for statistical computing. R Foundation for Statistical Computing, Vienna, Austria.

Reeves, J. C., B. C. Moon, M. J. Benton, and T. L. Stubbs. 2021. Evolution of ecospace occupancy by Mesozoic marine tetrapods. Palaeontology 64:31–49.

Revell, L. J. 2012. phytools: an R package for phylogenetic comparative biology (and other things). Methods in Ecology and Evolution 3:217–223.

Schulp, A. S., H. B. Vonhof, J. H. J. L. Van Der Lubbe, R. Janssen, and R. R. Van Baal. 2013. On diving and diet: resource partitioning in type-maastrichtian mosasaurs. Geologie en Mijnbouw/Netherlands Journal of Geosciences 92:165–170.

Skelton, P. W., R. A. Spicer, S. P. Kelley, and I. Gilmour. 2003. The Cretaceous world. Cambridge University Press, Cambridge.

Stayton, C. T. 2014. convevol: Quantifies and assesses the significance of convergent evolution. https://CRAN.R-project.org/package=convevol, accessed 29 April 2022.

Stayton, C. T. 2015. The definition, recognition, and interpretation of convergent evolution, and two new measures for quantifying and assessing the significance of convergence. Evolution 69:2140–2153.

Street, H. P. 2016. A re-assessment of the genus Mosasaurus (Squamata: Mosasauridae). University of Alberta, Edmonton, AB, Canada.

Strong, C. R. C., M. W. Caldwell, T. Konishi, and A. Palci. 2020. A new species of longirostrine plioplatecarpine mosasaur (Squamata: Mosasauridae) from the Late Cretaceous of Morocco, with a re-evaluation of the problematic taxon '*Platecarpus*' *ptychodon*. Journal of Systematic Palaeontology 18:1769–1804.

Stubbs, T. L., and M. J. Benton. 2016. Ecomorphological diversifications of Mesozoic marine reptiles: the roles of ecological opportunity and extinction. Paleobiology 42:547–573.

Tanaka, Y., and R. E. Fordyce. 2017. *Awamokoa tokarahi*, a new basal dolphin in the Platanistoidea (late Oligocene, New Zealand). Journal of Systematic Palaeontology 15:365–386.

Taylor, M. 1992. Functional anatomy of the head of the large aquatic predator *Rhomaleosaurus zetlandicus* (Plesiosauria, Reptilia) from the Toarcian (Lower Jurassic) of Yorkshire, England. Philosophical Transactions of the Royal Society of London B 335:247–280.

Thewissen, J. G. M., L. N. Cooper, J. C. George, and S. Bajpai. 2009. From land to water: the origin of whales, dolphins and porpoises. Evolution: Education and Outreach 2:272–288.

Uhen, M. D. 2010. The origin(s) of whales. Annual Review of Earth and Planetary Sciences 38:189–219.

Uhen, M. D. 2018. Basilosaurids and kekenodontids. Pp. 78–80 in Encyclopedia of Marine Mammals. 3rd ed. Academic, London.

Vermeij, G. J., and R. Motani. 2018. Land to sea transitions in vertebrates: the dynamics of colonization. Paleobiology 44:237–250.

Voss, M., M. S. M. Antar, I. S. Zalmout, and P. D. Gingerich. 2019. Stomach contents of the archaeocete *Basilosaurus isis*: apex predator in oceans of the late Eocene. PLoS ONE 14:1–24.

Watanabe, J., D. J. Field, and H. Matsuoka. 2021. Wing musculature reconstruction in extinct flightless auks (*Pinguinus* and *Mancalla*) reveals incomplete convergence with penguins (Spheniscidae) due to differing ancestral states. Integrative Organismal Biology 3:obaa040.

Young, M. T., S. L. Brusatte, M. B. de Andrade, J. B. Desojo, B. L. Beatty, L. Steel, M. S. Fernández, M. Sakamoto, J. I. Ruiz-Omeñaca, and R. R. Schoch. 2012. The cranial osteology and feeding ecology of the metriorhynchid crocodylomorph genera *Dakosaurus* and *Plesiosuchus* from the late Jurassic of Europe. PloS one 7:e44985.

Zelditch, M. L., J. Ye, J. S. Mitchell, and D. L. Swiderski. 2017. Rare ecomorphological convergence on a complex adaptive landscape: body size and diet mediate evolution of jaw shape in squirrels (Sciuridae). Evolution 71:633–649.